Bull. Mater. Sci., Vol. 38, No. 7, December 2015, pp. 1843–1850. © Indian Academy of Sciences.

Synthesis of Co_9S_8 and CoS nanocrystallites using Co(II) thiosemicarbazone complexes as single-source precursors

AMOL S PAWAR and SHIVRAM S GARJE*
Department of Chemistry, University of Mumbai, Vidyanagari, Santacruz (East), Mumbai 400 098, India

MS received 20 June 2015; accepted 30 July 2015

Abstract. **Cubic Co_9S_8 and hexagonal CoS nanocrystallites were prepared by pyrolysis and solvothermal decomposition methods using $Co(LH)_2Cl_2$ and CoL_2 (where LH = thiosemicarbazones of furfuraldehyde, cinnamaldehyde and 4-fluoro-acetophenone) as single-source precursors. These nanocrystallites were characterized by powder X-ray diffraction, scanning electron microscopy, transmission electron microscopy (TEM), selected area electron diffraction, UV–Vis, PL and Raman spectroscopic techniques. From TEM images, the average grain size of as-prepared cobalt sulphide nanocrystallites was found to be 7–10 nm. Depending on experimental conditions, various morphologies such as spherical, pyramidal, hollow spheres, etc. are observed in the TEM images.**

Keywords. **Cobalt sulphide; single-source precursors; pyrolysis and solvothermal decomposition.**

1. Introduction

Nanomaterials have attracted a great attention of the researchers due to their interesting chemical and physical properties and potential technological applications.[1–7] Transition metal sulphide nanostructures have wide applications. Among these materials, cobalt sulphides are especially important because the Co-S bonds present in them have several forces and binding mechanisms that can form ionic bonds, covalent bonds and metallic bonds in molecule.[8] Cobalt sulphide exists in several phases, such as Co_4S_3, Co_9S_8, CoS, $Co_{1-X}S$, Co_3S_4, Co_2S_3 and CoS_2.[9,10] These are important materials due to their use as hydrosulphurization catalyst in magnetic devices.[11,12] Cobalt sulphide (CoS) is a semiconductor with bandgap of 0.9 eV, whereas, Co_3S_4 has optical bandgap of about 0.78 eV. Electrical resistivity of CoS is of the order 10^{-10} Ω cm.[13] Cobalt disulphide is metallic solid, which displays ferromagnetic properties with Curie temperature of about 120 K.[14] In the recent years cobalt sulphide has been used in many applications such as solar energy absorber,[15] in ultra-density magnetic recording,[16] as anodes for Li-ion batteries[17] and catalysts for hydrosulphurization or dehydroaromatization.[18,19]

Various methods have been adopted to prepare these types of materials. This includes arc discharge evaporation,[20] chemical vapour deposition,[21] template confined growth,[22,23] hydrothermal processing,[24,25] etc. However, the preparation of CoS and Co_9S_8 using single-source precursor has not been much explored. In view of inherent advantages of single-source precursors, such as low toxicity, control over stoichiometries, limited pre-reactions etc., we thought it worthwhile to explore the possibility of use of cobalt thiosemicarbazone complexes as single-source precursors to get these materials. It is found that the thermal and solvothermal decomposition of thiosemicarbazone complexes of the type CoL_2 and $Co(LH)_2Cl_2$ (where LH = thiosemicarbazone of furfuraldehyde (furtsczH), cinnamaldehyde (cinnamtsczH) and 4-fluoroacetophenone (4-f-acphtsczH)) results into the formation of CoS or Co_9S_8 nanocrystallites (tables 1 and 2).

2. Experimental

2.1 *Instrumentation*

Elemental analyses (C, H, N, S) of all the compounds were carried out using Thermo Finnigan, Italy, Model FLASH EA 1112 Series, elemental analyzer. Infrared spectra of complexes were recorded using Perkin Elmer Spectrum One FTIR Spectrometer in 4000–400 cm^{-1} range. The molar conductance of the complexes of the solutions in dimethylformamide (10^{-3} mol l^{-1}) at room temperature was measured using Toshniwal conductivity meter. The TGA was carried out using Perkin Elmer Instrument, Pyris Diamond TG/DTA model, with heating rate of 10°C min^{-1} under nitrogen atmosphere. XRD studies were carried out using CuKα radiation on an Xpert PRO Analytical X-ray Diffractometer. SEM images were recorded on a FEI Quanta-200 scanning electron microscope at an accelerating voltage of 20 kV. EDS was performed with a spectroscope attached to SEM. Transmission electron microscopy (TEM) measurement and energy dispersive analysis by X-ray (EDAX) were recorded on a PHILIPS CM 200 microscope with operating voltages between 20 and 200 kV. The electronic spectra were recorded on a UV-2450 PC Shimadzu spectrometer in 800–200 nm

*Author for correspondence (ssgarje@chem.mu.ac.in, ssgarje@yahoo.com)

Table 1. Pyrolysis of CoL_2 and $CoCl_2(LH)_2$ complexes.

Precursors	Temperature (°C)	Crystalline phase	EDAX (Co:S)
$Co(furtscz)_2$	450	Hexagonal CoS (JCPDS: 75-0605)	46.15:53.85
$CoCl_2(furtsczH)_2$	475	Cubic Co_9S_8 (JCPDS: 75-2023)	48.48:51.52
$Co(cinnamtscz)_2$	425	Hexagonal CoS (JCPDS: 75-0605)	54.58:45.42
$CoCl_2(cinnamtsczH)_2$	500	Cubic Co_9S_8 (JCPDS: 75-2023)	61.41:38.59
$Co(4\text{-f-acphtscz})_2$	475	Cubic Co_9S_8 (JCPDS: 75-2023)	57.82:42.18
$CoCl_2(4\text{-f-acphtsczH})_2$	475	Cubic Co_9S_8 (JCPDS: 75-2023)	51.05:48.95

Table 2. Solvothermal decomposition of CoL_2 and $CoCl_2(LH)_2$ complexes in ethylene glycol.

Precursors	Crystalline phase	EDAX (Co:S)
$Co(furtscz)_2$	Cubic Co_9S_8 (JCPDS: 75-2023)	47.52:52.48
$CoCl_2(furtsczH)_2$	Hexagonal CoS (JCPDS: 75-0605)	47.17:52.83
$Co(cinnamtscz)_2$	Hexagonal CoS (JCPDS: 75-0605)	45.47:54.53
$CoCl_2(cinnamtsczH)_2$	Hexagonal CoS (JCPDS: 75-0605)	49.97:50.03
$Co(4\text{-f-acphtscz})_2$	Hexagonal CoS (JCPDS: 75-0605)	54.00:46.00
$CoCl_2(4\text{-f-acphtsczH})_2$	Hexagonal CoS (JCPDS: 75-0605)	50.94:49.03

range. Raman spectra were recorded on RENISHAW inVia Raman Microscope using 514 nm Argon ion laser in the range of 100–1200 cm^{-1}.

2.2 *Preparation of complexes*

The precursors were prepared as described below:

2.2a *Preparation of Co(furtscz)$_2$ (1)*: $Co(acac)_2{\cdot}4H_2O$ (0.7687 g, 3.08 mmol) was dissolved in 15 ml dry methanol. To this, 1.0533 g (6.22 mmol) of furfuraldehyde thiosemicarbazone dissolved in 10 ml dry methanol was added with constant stirring and the reaction mixture was refluxed for 8 h. Then it was cooled to room temperature and the solvent was evaporated under vacuum. The resulting brown solid was repeatedly washed with cyclohexane and n-hexane. The product obtained was dried *in vacuo* and weighed (yield: 1.032 g, 84.62%, M.P. 196°C). Elemental analyses for $CoC_{12}H_{12}N_6S_2O_2$, % found (calcd): Co 15.29 (14.91), C 36.81 (36.44), H 3.40 (3.03), N 21.73 (21.25), S 16.55 (16.19); IR: 3427 cm^{-1}, 3332 cm^{-1} (υ_{NH2} asym. and sym.), 1585 cm^{-1} (υ_{C-N}), 1013 cm^{-1} (υ_{C-S}); NMR (δ in ppm) ^{1}H: 6.54–8.43 (m, NH_2+ C_4H_3), ^{13}C: 178.66 (C=S), 149.30 (CH=N), 144.66, 135.61, 118.98, 113.30 (aromatic carbons).

2.2b *Preparation of CoCl$_2$ (furtsczH)$_2$ (2)*: To a round-bottom flask containing 0.7837 g (4.63 mmol) of furfuraldehyde thiosemicarbazone dissolved in 20 ml dry methanol, 0.5434 g (2.58 mmol) $CoCl_2{\cdot}6H_2O$ in methanol was added with constant stirring and stirring was continued for 24 h. Then the solvent was evaporated *in vacuo* to get a brown solid. It was repeatedly washed with cyclohexane and n-hexane to remove any impurities present. It was dried under vacuum to get a free solid (yield: 0.9802 g, 91.67%, M.P. 198°C). Elemental analyses for $CoCl_2C_{12}H_{14}N_6S_2O_2$ (%) found (calcd): Co 12.10 (12.58), C 30.60 (30.75), H 2.78 (2.99), N 17.65 (17.94), S 13.14 (13.67), Cl 15.28 (15.14); IR: 3384 cm^{-1}, 3270 cm^{-1} (υ_{NH2} asym. and sym.), 3125 cm^{-1} (υ_{N-H}), 1565 cm^{-1}(υ_{C-N}), 1022 cm^{-1} (υ_{C-S}); NMR (δ in ppm) ^{1}H: 6.57–7.92 (m, NH_2 + C_4H_4), 11.35 (s, NH), ^{13}C: 180.39 (C=S), 148.82 (CH=N), 146.15, 136.97, 120.10, 114.00 (aromatic carbons).

2.2c *Preparation of Co(cinnamtscz)$_2$ (3)*: To 0.6694 g (2.68 mmol) of $Co(acac)_2{\cdot}4H_2O$, dissolved in 15 ml dry methanol, 1.1166 g (5.43 mmol) of cinnamaldehyde thiosemicarbazone dissolved in 20 ml dry methanol was added with constant stirring. The reaction mixture was refluxed for 8 h. After the reaction was over, the solvent was evaporated under vacuum and the resulting brown solid was repeatedly washed with cyclohexane and n-hexane. The product obtained was dried *in vacuo* and weighed (yield: 1.025 g, 85.41%, M.P. 215°C). Elemental analyses for $CoC_{20}H_{20}N_6S_2$ (%) found (calcd): Co 12.37 (12.60), C 52.01 (51.83), H 4.53 (4.27), N 18.23 (17.96), S 14.05 (13.68); IR: 3450 cm^{-1}, 3319 cm^{-1} (υ_{NH2} asym. and sym.), 1573 cm^{-1}(υ_{C-N}), 1026 cm^{-1} (υ_{C-S}); NMR (δ in ppm) ^{1}H: 6.82–7.91 (m, NH_2 + C_6H_5–CH=CH–CH=N), ^{13}C: 177.72 (C=S), 151.29 (CH=N), 142.55, 139.26 (CH=CH), 129.46, 127.72, 123.65, 121.15 (aromatic carbons).

2.2d *Preparation of CoCl$_2$ (cinnamtsczH)$_2$ (4)*: To a round-bottom flask containing 0.7783 g (3.79 mmol) of cinnamaldehyde thiosemicarbazone dissolved in 20 ml dry

methanol, 0.4401 g (1.84 mmol) $CoCl_2{\cdot}6H_2O$ in methanol was added with constant stirring and stirring was continued for 24 h. Then the solvent was evaporated *in vacuo* to get a green solid. It was repeatedly washed with cyclohexane and n-hexane to remove any impurities present and then dried under vacuum to get free solid (yield: 0.6359 g, 62.87%, M.P. 215°C). Elemental analyses for $CoC_{20}H_{22}N_6S_2Cl_2$ (%) found (calcd): Co 11.11 (10.90), C 44.01 (44.40), H 4.53 (4.07), N 14.95 (15.04), S 11.32 (11.84), Cl 13.44 (13.11); IR: 3375 cm^{-1}, 3301 cm^{-1} (υ_{NH2} asym. and sym.), 3188 cm^{-1} (υ_{N-H}), 1579 cm^{-1} (υ_{C-N}), 989 cm^{-1} (υ_{C-S}); NMR (δ in ppm) ^{1}H 6.77–7.78 (m, NH_2 + C_6H_5–CH=CH–CH=N), 11.01 (s, NH), ^{13}C: 176.82 (C=S), 145.59 (CH=N), 139.64, 136.16 (CH=CH), 129.52, 128.47, 127.56, 125.46 (aromatic carbons).

2.2e *Preparation of Co(4-f-acphtscz)$_2$ (5)*: $Co(acac)_2{\cdot}4H_2O$, 0.6699 g (2.68 mmol), was dissolved in 15 ml dry methanol. To this, 1.1401 g (5.39 mmol) of 4-fluoro-acetophenone thiosemicarbazone dissolved in 25 ml dry methanol was added with constant stirring and the reaction mixture was refluxed for 8 h. After the reaction was over, the solvent was evaporated under vacuum and the resulting brown solid was repeatedly washed with cyclohexane and n-hexane. The product obtained was dried *in vacuo* and weighed (yield: 1.023 g, 79.39%, M.P. 135°C). Elemental analyses for $CoC_{18}H_{18}N_6S_2F_2$ (%) found (calcd): Co 12.46 (12.29), C 45.34 (45.08), H 3.70 (3.78), N 17.20 (17.52), S 13.11 (13.37); IR: 3417 cm^{-1}, 3275 cm^{-1} (υ_{NH2} asym. and sym.), 1598 cm^{-1} (υ_{C-N}), 1015 cm^{-1} (υ_{C-S}); NMR (δ in ppm) ^{1}H: 6.82–7.91 (s, NH_2, m, C_6H_5–C=N), ^{13}C: 177.73 (C=S), 142.89 (CH=N), 134.53, 130.39, 129.154, 127.80 (aromatic carbons).

2.2f *Preparation of $CoCl_2$(4-f-acphtsczH)$_2$ (6)*: To a round-bottom flask containing 0.8040 g (3.80 mmol) of 4-f-acetophenone thiosemicarbazone dissolved in 25 ml dry methanol, 0.4456 g (1.87 mmol) $CoCl_2{\cdot}6H_2O$ in methanol was added with constant stirring and stirring was continued for 24 h. The solvent was evaporated *in vacuo* when a green solid was obtained. It was repeatedly washed with cyclohexane and n-hexane to remove any impurities present and then dried under vacuum to get free solid (yield: 0.9210 g, 89.07%, M.P. 250°C). Elemental analyses for $CoC_{18}H_{20}N_6S_2F_2Cl_2$ (%) found (calcd): Co 11.19 (10.66), C 39.25 (39.09), H 3.80 (3.61), N 15.06 (15.20), S 11.31 (11.50), Cl 13.15 (12.83); IR: 3437 cm^{-1}, 3304 cm^{-1} (υ_{NH2} asym. and sym.), 3146 cm^{-1} (υ_{N-H}), 1598 cm^{-1}(υ_{C-N}), 1011 cm^{-1} (υ_{C-S}); NMR (δ in ppm) ^{1}H: 7.138–8.215 (m, NH_2 + C_6H_5), 10.038 (s, NH) ^{13}C: 176.10 (C=S), 148.05 (CH=N), 134.42, 129.52, 115.70, 115.42 (aromatic carbons).

2.3 *Thermal decomposition studies*

2.3a *Pyrolysis in a furnace*: Weighed quantities of each precursor (**1**–**6**, 350 mg) were taken in a quartz boat in a furnace. The furnace was heated to desired temperature under the flowing nitrogen atmosphere for 3 h. After cooling the furnace, residue in quartz boat was taken out and further it was characterized by XRD, SEM, TEM, EDAX, UV–Vis, PL and Raman spectra.

2.3b *Solvothermal decomposition in ethylene glycol*: Cobalt sulphide nanoparticles were prepared by refluxing 0.250 g of the each precursor (**1**–**6**) in 20 ml of ethylene glycol in 100 ml round-bottom flask under nitrogen atmosphere for 3 h. The colour of reaction mixture was changed to black. A viscous black solution with suspended particles was formed. After the decomposition is over the reaction mixture was brought to room temperature. The nanoparticles formed were separated by centrifugation. Most of the solid product was recovered by addition of methanol. The particles thus obtained were washed repeatedly with methanol and dried under vacuum. They were then characterized by XRD, SEM, TEM, EDAX, UV–Vis, PL and Raman spectra.

3. Results and Discussion

The precursors were prepared by reacting thiosemicarbazone ligands, LH (LH = thiosemicarbazones of furfuraldehyde, cinnamaldehyde and 4-F-acetophenone) either with $Co(OOCCH_3)_2{\cdot}4H_2O$ or $CoCl_2{\cdot}6H_2O$. The reactions of $Co(OOCCH_3)_2{\cdot}4H_2O$ with thiosemicarbazone ligands gave complexes of the type CoL_2 (**I**) (equation 1). However, simple addition reaction of $CoCl_2{\cdot}6H_2O$ with these ligands resulted in the formation of $CoCl_2(LH)_2$ adducts (**II**) (equation 2).

$$Co(OOCCH_3)_2{\cdot}4H_2O + 2LH \xrightarrow[-2CH_3COOH,\ -4H_2O]{\text{Dry methanol, reflux}} CoL_2 \quad (1)$$

$$CoCl_2{\cdot}6H_2O + 2LH \xrightarrow[-6H_2O]{\text{Dry methanol, R.T.}} CoCl_2(LH)_2 \quad (2)$$

These compounds were characterized by elemental analysis, IR, NMR (^{1}H and ^{13}C{^{1}H}) spectroscopy. In the IR spectra, the bands observed in the range of 3400–3200 cm^{-1} are assigned to NH_2 asymmetric and symmetric stretching modes. The N–H stretching mode is observed in IR spectrum of (**II**). This mode is absent in the spectrum of precursors (**I**), indicating deprotonation of the ligand in the complexes. The bands due to υ_{C-N} and υ_{C-S} are observed at 1583 and 1013 cm^{-1} for precursors (**I**) and 1619 and 1022 cm^{-1} for precursors (**II**), respectively. The values are shifted to lower wavenumbers compared to those in the spectra of free ligands.

In the ^{1}H spectrum of precursors (**II**) signal due to proton of –NH group is observed. This peak is absent in the spectrum of precursors (**I**), showing deprotonation of –NH group during the reaction. These observations are consistent

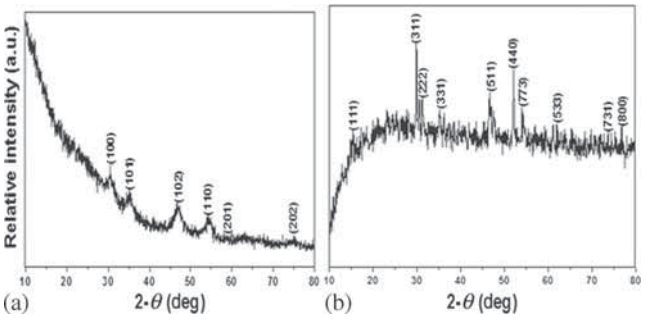

Figure 1. XRD patterns of (**a**) CoS and (**b**) Co_9S_8 nanocrystallites obtained from pyrolysis of $Co(furtscz)_2$ and $CoCl_2(furtsczH)_2$ in furnace at 450 and 475°C, respectively.

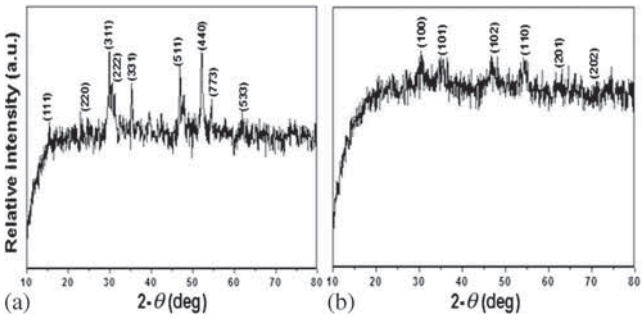

Figure 2. XRD patterns of (**a**) Co_9S_8 and (**b**) CoS nanocrystallites obtained from solvothermal decomposition of $Co(furtscz)_2$ and $CoCl_2(furtsczH)_2$ in ethylene glycol, respectively.

with ligand coordination through azomethine nitrogen and sulphur atoms. The molar conductivity was measured for all the precursors (**1**–**6**) in DMF (10^{-3} mol l^{-1}). These values are 7.5 (**1**), 8.0 (**2**), 7.65 (**3**), 13.8 (**4**), 12.31 (**5**) and 7.0 (**6**) Ω^{-1} cm^2 mol^{-1}, respectively. They are consistent with their non-electrolytic nature of the precursors.[26]

Pyrolysis of these complexes were carried out in furnace under nitrogen atmosphere. The black powder obtained was further characterized by powder XRD, SEM, TEM, SAED, UV–Vis, PL and Raman spectra. The pyrolysis of precursors (**1**) and (**2**) was carried out at 450 and 475°C, respectively. In both the cases black residue was obtained. The XRD pattern revealed that the decomposition of precursor (**1**) results in the formation of hexagonal CoS (JCPDS: 75-0605; figure 1a) and that of the precursor (**2**) gave cubic Co_9S_8 (JCPDS: 75-2023; figure 1b). No other diffraction peaks due to impurities were detected indicating that the synthesized product is pure. The average grain size (D) was calculated using Scherer formula $D = 0.89\lambda/\beta \cos\theta$, where $\lambda = 1.54060$ Å (CuKα) and β is FWHM at the diffraction angle θ. In the case of CoS calculated size is 7.0 nm, whereas for Co_9S_8 it is found to be 9.0 nm. The decompositions of precursors (**3**) and (**4**) were carried out at 425 and 500°C, respectively, whereas those of precursors (**5**) and (**6**) were carried out at 475°C. From the XRD of the materials obtained from these precursors it is found that precursor (**3**) resulted into hexagonal CoS formation, whereas precursors (**4**), (**5**) and (**6**) resulted into formation of cubic Co_9S_8 (supplementary figures S1 and S2).

The solvothermal decompositions of these precursors were carried out in ethylene glycol. Use of ethylene glycol like polyols can control the growth rate of crystal faces of metal sulphide (CoS) nanostructures and influence the oriented growth by interacting with these faces via adsorption and desorption reactions.[27] This growth mechanism is similar to CdS nanostructures in ethylenediamine.[28,29] Figure 2a shows XRD pattern of Co_9S_8 (JCPDS: 75-2023) obtained from solvothermal decomposition of precursor (**1**) in ethylene glycol and figure 2b shows XRD pattern of CoS (JCPDS: 75-0605) obtained from solvothermal decomposition of precursor (**2**) in ethylene glycol. The particle size calculated using Scherer formula is 4.0 nm for Co_9S_8 and 10.0 nm for CoS. The solvothermal decomposition of remaining precursors, i.e., (**3**–**6**) resulted into the formation of hexagonal CoS (JCPDS: 75-0605; supplementary figures S3 and S4). The crystallite sizes calculated for these materials vary from 3 to 5 nm.

The morphologies of the as-prepared materials were determined using SEM and TEM techniques. Figure 3a and b shows the SEM images of the materials obtained by pyrolysis of precursors (**1**) and (**2**), respectively, whereas figure 3c and d shows the EDAX spectra of the respective materials. SEM of the material obtained from precursor (**1**) shows the formation of flake-like morphology. Precursor (**2**) also gave material with the same morphology, but with smaller particle size. The EDAX analysis of both the materials matches with the 1:1 ratio of Co and S. The SEM images and EDAX spectra of the materials obtained by pyrolysis of precursors (**3**–**6**) are shown in supplementary figures S5 and S6. The morphology of the materials obtained is similar to the materials obtained from precursors (**1**) and (**2**). The EDAX analysis matches with the presence of 1:1 ratio of Co and S.

Figure 4 shows the SEM image and EDAX spectra of the materials obtained by solvothermal decomposition of precursors (**1**) and (**2**). The morphology of the materials obtained from these precursors is found to be nearly spherical particles. The EDAX analysis tentatively matches with 1:1 ratio between Co and S. The SEM images of the materials obtained by solvothermal decomposition of precursors (**3**–**6**) are given in supplementary figures S7 and S8. The morphologies of the materials are found to be flake like. The EDAX analysis of all these materials matches with 1:1 stoichiometries between Co and S.

Figure 5 shows TEM images and SAED patterns of the nanocrystals obtained by pyrolysis of precursors (**1**) and (**2**), whereas supplementary figures S9 and S10 show TEM images and SAED patterns of the materials obtained from pyrolysis of precursors (**3**–**6**). The SAED pattern contains well-defined rings suggesting the presence of highly crystalline materials. In SAED pattern of CoS nanocrystallites, the measured spacing of the crystallographic planes are 0.291 and 0.168 nm corresponding to the two characteristics planes at 100 and 110 (figure 5c). The SAED pattern of Co_9S_8 obtained from pyrolysis of precursor (**2**) shows 0.285,

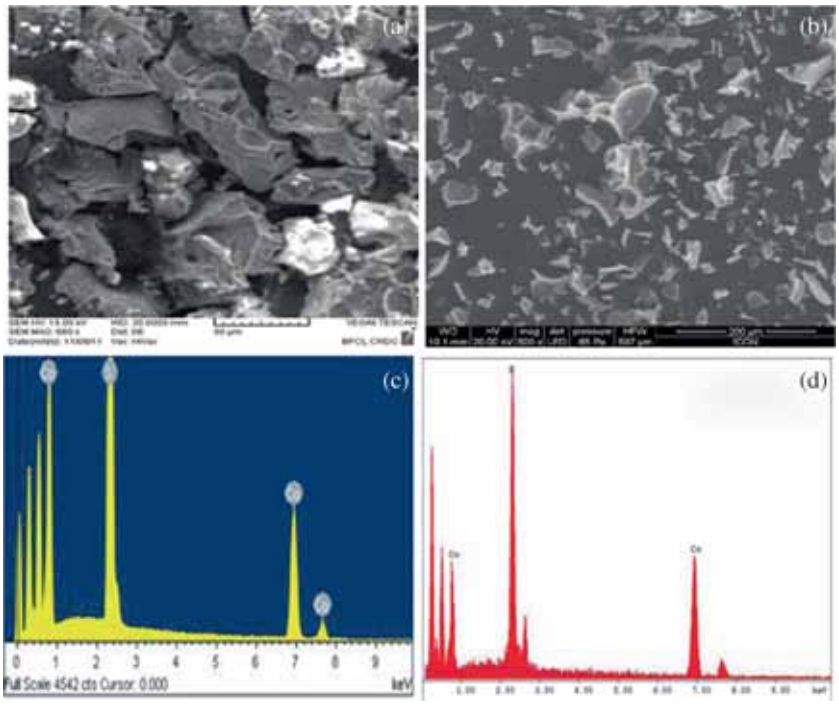

Figure 3. SEM images and EDAX spectra of (**a**, **c**) CoS and (**b**, **d**) Co_9S_8 nanocrystallites obtained from pyrolysis of $Co(furtscz)_2$ and $CoCl_2(furtsczH)_2$ in furnace at 450 and 475°C, respectively.

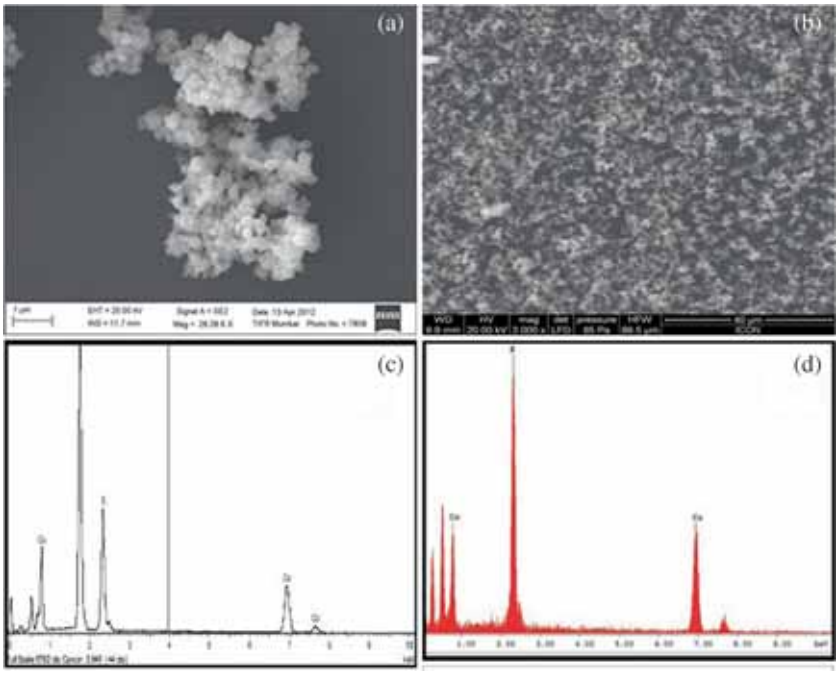

Figure 4. SEM images and EDAX spectra of (**a**, **c**) Co_9S_8 and (**b**, **d**) CoS nanocrystallites obtained from solvothermal decomposition of $Co(furtscz)_2$ and $CoCl_2(furtsczH)_2$ in ethylene glycol, respectively.

0.190 and 0.175 nm d-spacings corresponding to 222, 511 and 440 planes (figure 5d). The spherical shape morphology can be seen in TEM image. The TEM images for pyrolysis of precursors (**4**) and (**6**) show pyramidal and spherical shape morphology, respectively. (supplementary figures S9 and S10).

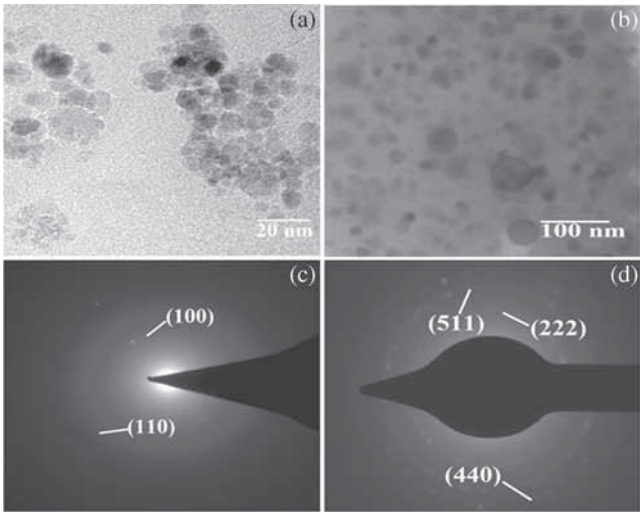

Figure 5. TEM images and SAED patterns of (**a**, **c**) CoS and (**b**, **d**) Co_9S_8 nanocrystallites obtained from pyrolysis of $Co(furtscz)_2$ and $CoCl_2(furtsczH)_2$ in furnace at 450 and 475°C, respectively.

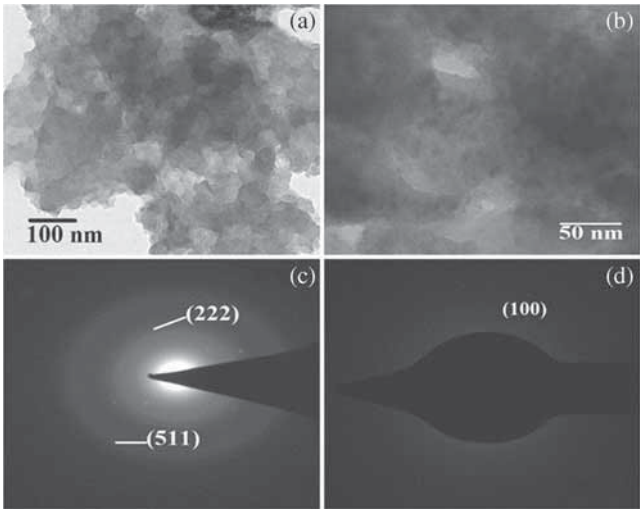

Figure 6. TEM images and SAED patterns of (**a**, **c**) CoS and (**b**, **d**) Co_9S_8 nanocrystallites obtained from solvothermal decomposition of $Co(furtscz)_2$ and $CoCl_2$ $(furtsczH)_2$ in ethylene glycol, respectively.

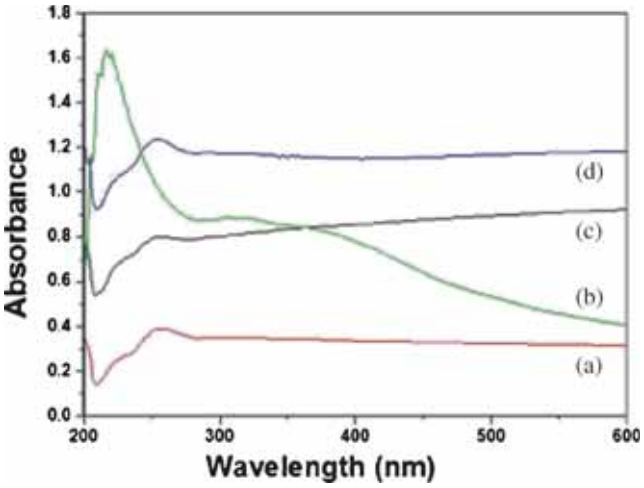

Figure 7. Absorption spectra of (**a**) Co_9S_8 nanocrystallites obtained from pyrolysis of $CoCl_2(furtsczH)_2$, (**b**) CoS nanocrystallites obtained from pyrolysis of $Co(cinnamtscz)_2$, (**c**) CoS nanocrystallites obtained from solvothermal decomposition of $CoCl_2(furtsczH)_2$ and (**d**) CoS nanocrystallites obtained from solvothermal decomposition of $CoCl_2(4\text{-}facphtsczH)_2$.

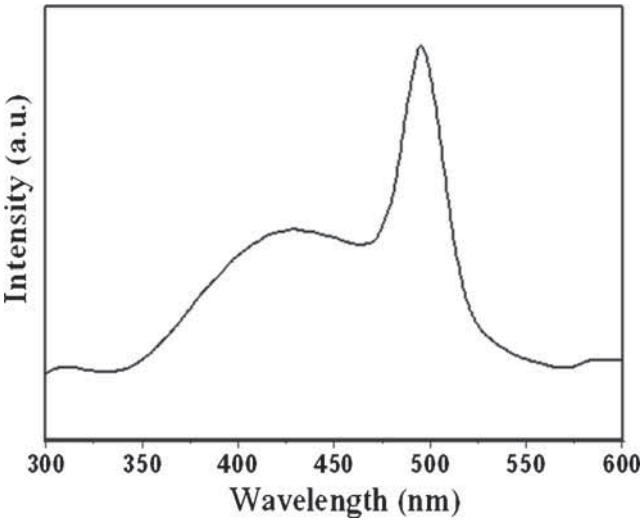

Figure 8. PL spectrum of CoS nanocrystallites obtained from solvothermal decomposition of $Co(cinnamtscz)_2$ in ethylene glycol.

Figure 6 shows the TEM images of CoS and Co_9S_8 nanoparticles obtained from the solvothermal decomposition of precursors (**1**) and (**2**). The spherical shape morphology can be seen in TEM image with agglomeration of nanoparticles. The SAED pattern of these nanocrystallites shows the amorphous nature. The TEM images of the materials obtained by solvothermal decomposition of precursors (**3**) and (**4**) show the formation of hollow sphere and cotton-like spherical shape morphology of these materials (supplementary figure S11). Supplementary figure S12 shows TEM images and the SAED patterns of the materials obtained from precursors (**5**) and (**6**). The formation of spongy morphology nanoparticles is observed in their TEM images. The rings present in the SAED patterns reveal crystalline nature of these materials.

UV–Vis absorption spectra of Co_9S_8 and CoS nanocrystallites dispersed in methanol are shown in figure 7. Figure 7a and b shows spectra for Co_9S_8 obtained from the pyrolysis of precursor (**2**) and CoS obtained from precursor (**3**). Figure 7c and d shows spectra of the material (CoS) obtained by solvothermal decomposition of precursors (**2**) and (**6**). In the absorption spectra of these materials, an absorption band at 251 nm is observed for CoS and 255 nm for Co_9S_8 nanocrystallites, which are blue shifted as compared to bulk CoS which shows absorption band at 347 nm. This indicates the formation of smaller particles.[30]

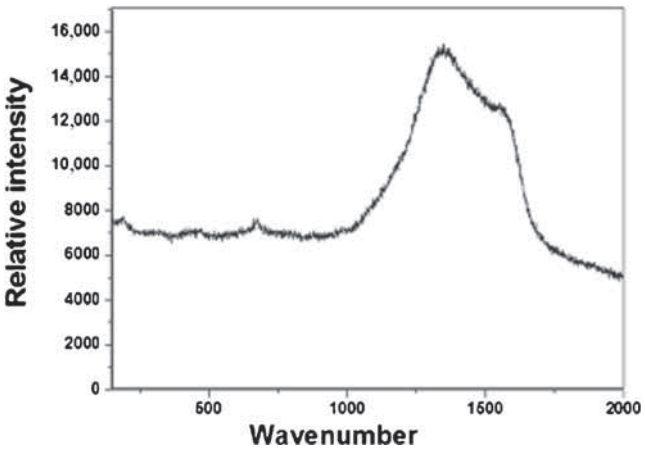

Figure 9. Raman spectrum of CoS nanocrystallites obtained from pyrolysis of $Co(furtscz)_2$ at 450°C.

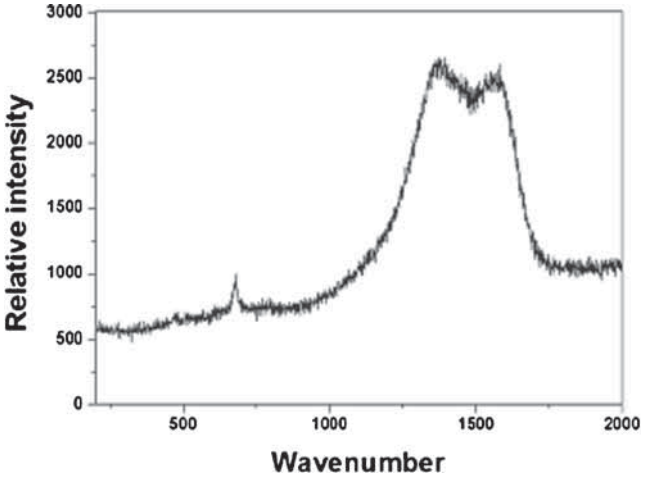

Figure 10. Raman spectrum of CoS nanocrystallites obtained from solvothermal decomposition of $CoCl_2(furtsczH)_2$ in ethylene glycol.

The representative photoluminescence spectrum of CoS nanocrystallites obtained from solvothermal decomposition of precursor **3** recorded at an excitation wavelength of 265 nm at room temperature is shown in figure 8. Cobalt is a transition metal impurity. It is a fast diffuser and gives rise to both radiative and nonradiative centres.[31] The PL spectrum consists of two bands, of which one broad violet emission peak is observed at 423 and another at 495 nm for CoS nanocrystallites obtained from solvothermal of $Co(cinnamtscz)_2$. Bhattacharjee and Lu[32] have reported 418 nm peaks to S^{2-} vacancy.[32–34] Yanagida *et al*[34] have observed defect-related longer wavelength luminescence at about 420 nm. It has been reported that 423 nm peak has been classically termed as self-activated luminescence and known to be due to the recombination of carriers between S vacancy-related donor and valance band. The strong blue peak observed at 495 nm may arise due to native point defects.

Raman spectroscopy is an effective method to study the structures of the materials. The Raman spectra of CoS nanocrystallites obtained from pyrolysis of precursor **(1)** and solvothermal decomposition of precursor **(2)** show three well-resolved peaks at 675, 1360 and 1560 cm^{-1} (figures 9 and 10). Similar Raman spectrum is observed for CoS nanocrystallites obtained from pyrolysis of precursor **(3)** (supplementary figure S13).

4. Conclusions

The hexagonal (CoS) and cubic (Co_9S_8) cobalt sulphide nanocrystallites were obtained by simple pyrolysis and solvothermal decomposition routes using single-source precursors, $Co(L)_2$ and $CoCl_2(LH)_2$. The presence of nanocrystallites was confirmed by XRD, SEM, TEM, SAED, UV–Vis, PL and Raman spectral data.

Acknowledgements

ASP thanks DST-PURSE for financial support. Thanks are due to SAIF, IIT Bombay, for TEM and SAED patterns and TIFR, Mumbai, for providing SEM and EDAX data.

Electronic Supplementary Material

Supplementary material pertaining to this article is available on the Bulletin of Materials Science website (www.ias.ac.in/matersci).

References

1. Schmid G 1994 *Cluster and colloids* (New York: VCH Press)
2. Furstner, A (ed) 1996 *Active metals* (Weinheim and New York: VCH)
3. Wang Y 1995 *Adv. Photochem.* **19** 179
4. Fenler J H and Meldrum E C 1997 *J. Cluster Sci.* **7** 607
5. Ozin G A 1992 *Adv. Mater.* **4** 612
6. Wells R L and Gladfelter W L 1997 *J. Cluster Sci.* **8** 217
7. Chow G M and Gonsalves K E 1996 *Am. Chem. Soc. Symp. Ser.* 622
8. Hu Q R, Wang S L, Zhang Y and Tang W H 2010 *J. Alloys Compd.* **498** 707
9. Wold A and Dwight K 1993 *Solid State Chemistry* (New York: Chapman and Hall Inc.)
10. Rao C N R and Pisharody K P R 1976 *Prog. Solid State Chem.* **10** 207
11. Wold A and Dwight K 1992 *J. Solid State Chem.* **96** 53
12. Pecararo T A and Chianelli R R 1981 *J. Catal.* **67** 430
13. Pathan H M and Lokhande C D 2004 *Bull. Mater. Sci.* **2** 85
14. Morris B, Johnson V and Wold A 1967 *J. Phys. Chem. Solid* **28** 1565
15. Smith G B, Ignatiev A and Zajac G 1980 *J. Appl. Phys.* **51** 4186

16. Whitney T M, Jiang J S, Searson P and Chien C 1993 *Science* **261** 1316
17. Yue G H, Yan P X, Fan X Y, Wang M X, Qu D M, Wu Z G, Li C and Yan D 2007 *Electrochem. Solid State Lett.* **10** 29
18. Feng Y G, He T and Vante N A 2008 *Chem. Mater.* **20** 26
19. Chen X Y, Zhang Z J, Qiu Z G, Shi C W and Li X L 2007 *J. Colloid Interface Sci.* **308** 271
20. Chopra N G, Luyren R J, Cherry K, Crespi V H, Cohen V L, Louie S G and Zettle A 1995 *Science* **269** 966
21. Yang J, Liu Y C, Lin H M and Chen C C 2004 *Adv. Mater.* **16** 713
22. Goldberger J, He R, Zhang Y, Lee S, Yan H, Choi H J and Yang P 2003 *Nature* **422** 599
23. Wirtz M and Martin C R 2003 *Adv. Mater.* **15** 455
24. Li Y D, Wang J W, Deng Z X, Wu X Y, Sun X M, Yu D P and Yang P D 2001 *J. Am. Chem. Soc.* **123** 9904
25. Wang Z H, Wang L L and Wang H 2008 *Cryst. Growth Des.* **8** 4415
26. Geary W J 1971 *Coord. Chem. Rev.* **7** 81
27. Hu Q R, Wang S L, Zhang Y and Tang H 2010 *J. Alloys Compd.* **491** 707
28. Wang Q, Gang X and Han G R 2005 *J. Solid State Chem.* **178** 2680
29. Zhao Q T, Hou L S, Huang R A and Li S Z 2003 *Inorg. Chem. Commun.* **6** 1459
30. Khaorapapong N, Ontam A and Ogawa M 2011 *Appl. Clay Sci.* **51** 182
31. Pal D and Bose D N 1994 *Bull. Mater. Sci.* **20** 401
32. Bhattacharjee B and Lu C H 2006 *Thin Solid films* **514** 132
33. Yang F, Wilkinson M, Austin E J and O'Donnel K P 1993 *Phys. Rev. Lett.* **70** 323
34. Yanagida S, Yoshida M, Shiragami T, Pac C, Mori H and Fujita H 1990 *J. Phys. Chem.* **94** 3104